Transactions of the Materials Research Society of Japan 28 [2] 461-464 (2003)

Synthesis of Sulfur-doped TiO_2 by Ion Implantation

Tsutomu Umebayashi[†], Tetsuya Yamaki[‡], Syunya Yamamoto[‡],
Sigeru Tanaka[‡] and Keisuke Asai[†]
[†]Department of Quantum Engineering and Systems Science, Graduate School of Engineering, The University of Tokyo,
7-3-1 Hongo, Bunkyo-ku, Tokyo 113-8656, Japan
Fax: 81-03-5841-6978, e-mail: asai@q.t.u-tokyo.ac.jp
[‡]Department of Materials Development, Takasaki Radiation Chemistry Research Establishment, Japan Atomic Energy
Research Institute (JAERI), 1233 Watanuki, Takasaki, Gunma 370-1292, Japan
Fax: 81-027-346-9687

Sulfur-doped titanium dioxide (TiO_2) was prepared by an ion implantation technique. Rutile TiO_2 single crystals were implanted with 200 keV S^+ at a fluence of 8×10^{15} ions/cm^2, and subsequently annealed in air. As assessed by the Rutherford backscattering spectrometry and channeling analysis, radiation damage recovered after annealing at 600 °C for 6 hours. In the implanted and annealed crystal, sulfur occupied the oxygen sites to form Ti–S bonds. The S^+ implantation caused the absorption edge of TiO_2 to be shifted into the lower energy region. Based on first principles band calculation, mixing of the S 3p states with the valence band was found to contribute to the bandgap narrowing.

Key words: TiO_2, Sulfur, Ion implantation, Photocatalyst, Electronic structure, Optical property

1. INTRODUCTION

Because of the pressing need to prevent and control the spread of pollutants in the air and water, photocatalytic methods have received much attention. Although titanium oxides (TiO_2) are a most promising photocatalytic material [1, 2], it is active only under ultraviolet (UV) light irradiation because of its wide bandgap (~3.0 eV) [3]. The effective utilization of visible (VIS) light, therefore, is one of the important subjects for the increased applicability of TiO_2 as a photocatalyst. In past studies, in order to improve the photocatalytic activity of TiO_2 and to extend its absorption edge into the VIS-light region, the doping of various transition metal cations has been intensively investigated [4-7]. Except for a few cases [6, 7], however, the photocatalytic activities of the cation-doped TiO_2 decreased even in the UV region. This is because the doped oxides suffer from a thermal instability or an increase in the carrier-recombination centers [4, 5].

Recently, some groups have demonstrated the substitution of a nonmetal atom such as nitrogen (N) [8-12] and fluorine (F) [13-15] for oxygen (O). Lee et al. [8] fabricated the N-doped TiO_2 films on a silicon substrate by metalorganic chemical vapor deposition using titanium tetra-isopropoxide and nitrous oxide. Asahi et al. [11, 12] showed that N-doping shifted the optical absorption edge to a lower energy, thereby increasing the photoreactivity in the VIS-light region. F-doping into TiO_2 was carried out by gas-phase HF treatment at high temperatures [13], a sol-gel technique [14] and ion implantation [15]. The photocatalytic performance of the F-doped oxides was enhanced due to reduction of the recombination rate of the photogenerated charge carriers [14]. These studies demonstrated that the doping with a nonmetal impurity can provide an effective modification of the electronic structures of TiO_2.

Although the substitution of sulfur (S) at the O sites could significantly modify the electronic structures of TiO_2 because S has a larger ionic radius compared to N and F, it was considered

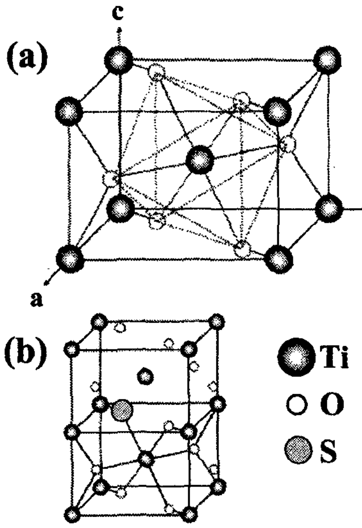

Fig. 1. (a) Primitive unit cell of rutile TiO_2 and the $[TiO_6]^{8-}$ octahedron (dotted-lines) with the O_h symmetry. (b) The super-cell model considered in the present work. Dark spheres: Ti; white spheres: O; gray sphere: S.

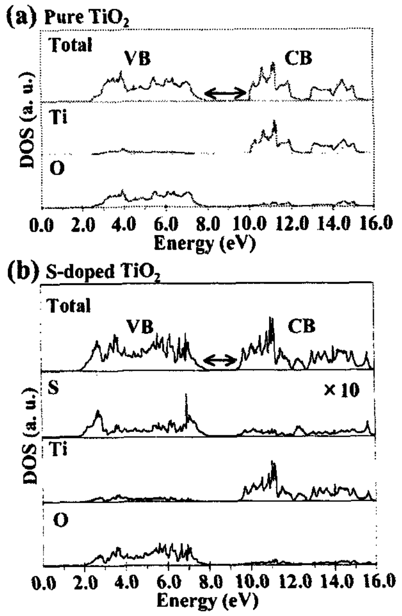

Fig. 2. Total and partial DOS of the (a) pure and (b) S-doped TiO_2.

that the conventional techniques, such as the sol-gel method, gas-phase treatment at high temperatures and physical or chemical deposition method etc., are hard to dope S into TiO_2 due to large formation energy required for the substitution of S for O [11]. Contrary to this expectation, the S-doped anatase TiO_2 polycrystalline powder, including S substituted for O, was synthesized by the oxidative heating of the TiS_2 powder [16]. Compared to the pure anatase, the optical absorption edge was shifted to a lower energy region in the S-doped anatase. We expect this S-doped TiO_2 to be available as a novel VIS-light photocatalyst material [17].

However, the oxidative heating of TiS_2 is a difficult method to control the concentration of the dopant and its dependant profile, which should govern the photocatalytic activities of the doped TiO_2. Control of these factors and introduction of a nonsoluble element into the host matrix can be best carried out by ion implantation. This is a well-known technique used to modify the properties of materials in the near surface region. In this study, the S-doping effects on the electronic structures of TiO_2 were analyzed by the first principles band calculation. Subsequently, the S-doped TiO_2 single crystal was synthesized by ion implantation and its optical properties and electronic structures were investigated.

2. CALCULATION AND EXPERIMENTAL METHODS

The electronic structures of the S-doped TiO_2 were examined using first principles band calculations with the super-cell approach. The primitive unit cell of TiO_2 in the rutile structure and the super-cell model considered in this study are shown in Figures 1 (a) and (b). Rutile TiO_2 has a tetragonal structure (P42/mmm space group, a = 4.594 Å, c = 2.959 Å) and contains 2 formula units in the unit cell. Our model consists of 2 unit-cells stacked along the c-axis, where one O atom was replaced by the S atom. The band calculations were carried out by the full potential linearized augmented plane wave (F-LAPW) method [18] based on the density functional theory [19] within the generalized gradient approximation [20]. These calculations were performed using the WIEN97 code developed by Blaha et al. [21]. In this calculation, the potentials are described by two kinds of basis sets: inside a non-overlapping atomic sphere with radii R_{MT}, the linear combination of a radial function times the spherical harmonics was used and in the interstitial region, a plane-wave function was used. The atomic sphere radii R_{MT} adopted for Ti, O and S were 1.9, 1.7 and 1.76 au, respectively. Inside the atomic sphere, the partial waves were expanded up to $l_{max} = 6$, while the number of plane waves in the interstitial was limited by the cut-off at $K_{max} = 8.0 / R_{MT}$. The number of plane-wave basis functions in the interstitial region of the S-doped and pure systems was about 600 and 3800, respectively. Integration in a reciprocal space was performed by the tetrahedron methods taking 30 k-points for the S-doped TiO_2 and 60 k-points for the pure TiO_2 in the first Brillouin zone. We determined the self-consistent potential and the charge density in the super-cell under these conditions.

Optically polished single-crystalline TiO_2 (rutile; 10 × 10 × 0.5 mm) with a <001> crystallographic axis was used for our experiments. The implantations were carried out with 200 keV S^+ at room temperature (RT). The implanted crystals were annealed at 600 °C in air for 6 hours. After the annealing, the Rutherford backscattering spectrometry and ion channeling analysis (RBS-C) measurements were performed with a 2 MeV $^4He^+$ beam from a 3 MV single-ended accelerator. The charge state of the dopants at the surface was investigated by x-ray photoelectron spectroscopy (XPS) with an ESCALAB-MK II (VG Scientific) using an Mg X-ray source (Mg Kα, $h\nu$ = 1253.6 eV). The differential absorption spectra were measured by a UV/VIS spectrophotometer.

3. RESULTS AND DISCUSSION

3.1 Calculation results

Figure 2 shows the calculated total and partial density of states (DOS) of the VB and CB for the pure and S-doped TiO_2. The electron density maps (EDMs) illustrated with projection onto the $(\bar{1}00)$ lattice planes for the VB are given in Figure 3.

According to the past studies on the electronic structures of the pure oxides [22, 23], the lowest bandgap of TiO_2 is located at a Γ point with the value of 1.93 eV. This bandgap energy is much smaller than that experimentally observed, 3.0 eV,

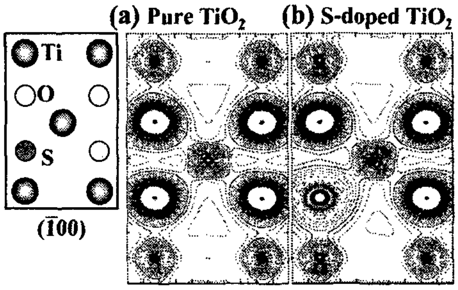

Fig. 3. Electron density maps for the valence band of the (a) pure and (b) S-doped TiO_2. Dark spheres: Ti; white spheres: O; gray sphere: Substitutional site.

due to the well-known shortcoming of the DFT using GGA [24]. As shown in Figure 2 (a), the VB and CB consist of both the Ti 3d and O 2p orbitals. Because the Ti 3d orbital is split into two parts, the t_{2g} and e_g states in an octahedron ligand field with O_h symmetry (see Fig. 1 (a)), the CB is divided into lower and upper parts.

When TiO_2 is doped with S, the S 3p states are somewhat delocalized, thus greatly contributing to the formation of the VB with the O 2p and Ti 3d orbitals (see Figs. 2 (b) and 3 (b)). Consequently, the mixing of the S 3p states with VB increases the width of the VB itself. This results in a decrease in the bandgap energy due to S doping. The calculated bandgap energies were 1.31 eV for the S-doped TiO_2 and 1.93 eV for the pure TiO_2. Our calculation results consistently confirm that the S atoms doped into the substitutional site of rutile TiO_2 are effective for the bandgap narrowing. This corresponds to our calculated results previously reported for the anatase TiO_2 [16].

TiO_2 doped with a transition metal, i.e., Cr, V, Mn, Fe, etc., also absorbs a photon in the VIS-light regions. This is caused by an impurity level in the bandgap [4, 23]. In contrast with the case of the transition metal doping, the bandgap narrowing leads to the optical-absorption in the VIS-light region for the S-doped TiO_2.

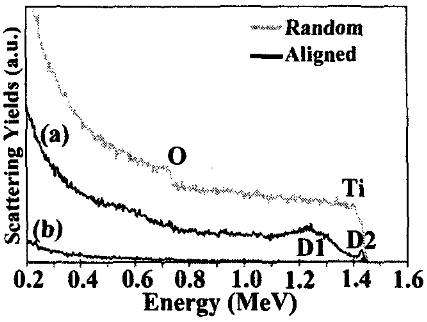

Fig. 4. 2 MeV $^4He^+$ RBS-C spectra of TiO_2 single crystals implanted with 200 keV S^+ (8×10^{15} ions/cm^2) at RT for (a) as implanted and (b) annealed samples at 600°C in air for 6 h. Gray lines: random spectra; black lines: <001> aligned spectra.

3.2 Experimental results

Figure 4 shows the random and <001> aligned RBS-C spectra after the implantation of 8×10^{15} S^+/cm^2 at RT. Based on the Rutherford universal manipulation program (RUMP) code [25], the signal of S occurs around 1.22 MeV. The S signals were not detected for the implanted crystal. As shown in the aligned spectrum of the as-implanted sample, two damage peaks (D1 and D2) were observed around 1.4 and 1.2 MeV and both of these did not reach the random level. The former peak is due to the surface damage, while the latter is attributed to the displacement damage in the solids generated by the S implantation. According to the RUMP simulation, the displacement damage lies at a depth of 220 nm. A large amount of S atoms would occur in a deeper area in the as-implanted crystal. The aligned spectrum of the sample annealed at 600 °C for 6 hours, where the damage peak disappeared, indicates that radiation damage decreased due to the annealing.

Figure 5 shows the XPS spectra for the S 2p core level of the (a) pure and (b) S-implanted crystal annealed at 600 °C for 6 hours. These spectra were referenced to the C 1s state at 284.8 eV. The S 2p state had a broad peak because of the overlap of the split sublevels, the $2p_{3/2}$ and $2p_{1/2}$ states, with separation of 1.2 eV by spin-orbit coupling [26]. Two peaks were observed around 168 eV and 160 eV for the implanted crystal. The higher-energy peak can be ascribed to the surface S atoms adsorbed as SO_2 molecules [17, 18], which were generated through the diffusion of the implanted S atoms. The signal at 160 eV is associated with S forming Ti-S bonds in the TiO_2.This signal is associated with S forming Ti-S bonds in the TiO_2 [17, 18]. A trace amount of S would remain in the annealed sample as substitutional atoms at the O sites.

Combining the above RBS-C and XPS results, we concluded that the S-doped TiO_2 was synthesized by the S implantation and subsequent annealing at 600 °C.

Figure 6 shows the differential absorption spectrum $\Delta A(\lambda)=-10\times\log(T/T_0)$, where T and T_0

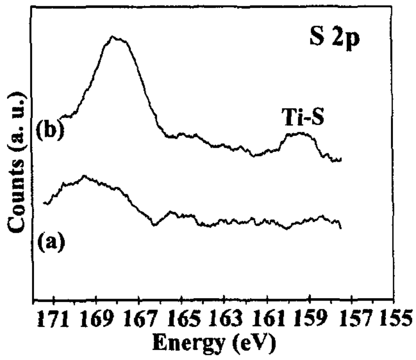

Fig. 5. X-ray photoelectron spectra for the S 2p state of the (a) pure and (b) S-implanted and subsequently annealed TiO_2.

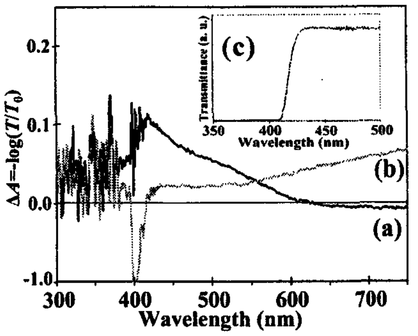

Fig. 6. Differential absorption spectrum for the (a) S-doped and (b) defective crystal ΔA=-log(T/T_0), where T and T_0 are the transmittance of the implanted and unimplanted crystal, respectively. (c) Transmittance spectrum of the undoped TiO_2 crystal.

are the transmittance of the implanted and unimplanted TiO_2 crystal, respectively. In the pure crystal, optical absorption is observed below 410 nm which corresponds to the bandgap energy [3] (Fig. 6 (c)). As shown in the spectrum (b) of a defective rutile crystal, which was implanted with 200 KeV Ar^+ at a fluence of 1×10^{16} ions/cm^2, the radiation defects induced absorption of VIS light. In contrast to this crystal, the S-doped crystal absorbed the light below 650 nm. This VIS light absorption would be due to the S-doping [16, 17] or O-vacancies [27].

4. CONCLUSION

We analyzed the electronic structures of the S-doped TiO_2 using the first principles band calculations. The S-doped crystals were prepared by ion implantation methods and its optical properties were examined by UV/VIS spectroscopy. The obtained results are summarized as follows:

(i) S-doping into TiO_2 causes an increase in the width of the valance band, resulting in bandgap narrowing.

(ii) S-doped TiO_2 was synthesized by 200 KeV S^+ implantation and subsequent thermal annealing at 600 °C in air for 6 hours.

(iii) In the S-doped TiO_2, the optical-absorption occurred in the visible light region.

References

[1] A. Fujishima and K. Honda, *Nature*, **238**, 37-38 (1972).

[2] D. F. Ollis and H. Al-Ekabi, Photocatalysis Purification and Treatment of Water and Air. Elsevier Sci. Pub, New York, (1993).

[3] J. Pascual and J. Camassel, H. Mathieu, *Phys. Rev. Lett.*, **39**, 1490-1493 (1977).

[4] W. Choi, A. Termin and M. R. Hoffmann, *J. Phys. Chem.*, **98**, 13669-13679 (1994).

[5] J. M. Herrmann, J. Disdier and P. Pichat, *Chem. Phys. Lett.*, **108**, 618-622 (1984).

[6] M. Anpo, Y. Ichihashi, M. Takeuchi and H. Yamashita, *Res. Chem. Intermed.*, **24**, 143-149 (1999).

[7] K. E. Karakitsou and X. E. Verykios, *J. Phys. Chem.*, **97**, 1184-1189 (1993).

[8] D. H. Lee, Y. S. Cho, W. I. Yi, T. S. Kim, J. K. Lee and H. J. Jung, *Appl. Phys. Lett.*, **66**, 815-816 (1995).

[9] N. C. Saha and H. G Tompkins, *J. Appl. Phys.*, **72**, 3072-3079 (1992).

[10] S. Sato, *Chem. Phys. Lett.*, **123**, 126-128 (1986).

[11] R. Asahi, T. Morikawa, T. Ohwaki, A. Aoki and Y. Taga, *Science*, **293**, 269-271 (2001).

[12] T. Morikawa, R. Asahi, T. Ohwaki, A. Aoki and Y. Taga, *Jpn. J. Appl. Phys.*, **40**, 561-563 (2001).

[13] S. N. Subbarao, Y. H. Yun, R. Kershaw, K. Dwinghta and A. Wold, *Inorg. Chem.*, **18**, 488-492 (1979).

[14] A. Hattori, M. Yamamoto, H. Tada and S. Ito, *Chem. Lett.*, 707-708 (1998).

[15] T. Yamaki, T. Sumita and S. Yamamoto, *J. Mater. Sci. Lett.*, **21**, 33-35 (2002).

[16] T. Umebayashi, T. Yamaki, H. Itoh and K. Asai, *Appl. Phys. Lett.*, **81**, 454-456 (2002).

[17] T. Umebayashi, T. Yamaki, S. Tanaka and K. Asai, *Chem. Lett.*, in press (2003).

[18] O. K. Andersen, *Phys. Rev.*, **B12**, 3060-3083 (1975).

[19] W. Kohn and L. J. Sham, *Phys. Rev.*, **140**, 1133-1138 (1965).

[20] J. P. Perdew, K. Burke and M. Ernzerhof, *Phys. Rev. Lett.*, **77**, 3865-3868 (1996).

[21] P. Blaha, K. Schwarz and J. Luitz, A Full Potential Linearized Augmented Plane Wave Package for Calculating Crystal Properties, Karlheinz Schwarz, Techn. Univ. Wien, Vienna, (1999).

[22] P. I. Sorantin and K. Schwarz, *Inorg. Chem.*, **31**, 567-576 (1992).

[23] T. Umebayashi, T. Yamaki, H. Itoh and K. Asai, *J. Phys. Chem. Solids*, **63**, 1909-1920 (2002).

[24] C. Stampfl and C. G. Van de Wall, *Phys. Rev.*, **B 59**, 5521-5535 (1999).

[25] L. R. Doolittle, *Nucl. Instr. and Meth. B*, **9** 344-351 (1985).

[26] B. J. Lindberg, K. Hamrin, G. Johansson, U. Gelius, A. Fahlman, C. Nordling and K. Siegbanh, *Phys. Scripta.*, **1**, 286-298 (1970).

[27] D. C. Cronemeyer, *Phys. Rev.*, **113**, 1222-1226 (1958).

(Received December 21, 2002; Accepted March 26, 2003)